Ion Bernstein Mode Instability with Ring Velocity Distribution Function

N. Noreen[1],F. Riaz[1], S. Malik[1],S. Zaheer[1]
1 : Forman Christian College (A Chartered University), Lahore, Pakistan

Abstract

The Bernstein mode instability plays a vital role in tokamak and in space plasma regimes like Jovian planets and interstellar spaces. In the present manuscript, we have introduced the contribution of Ions along with electrons with the help of ring velocity distribution function. We have concluded that the ions play a significant role in shifting the threshold frequency value towards lower wavelength regime. On comparison with electron Bernstein mode, it is concluded that the electron mode becomes unstable for higher wavelength but on contrary ion Bernstein mode tries to be more stable at low frequency. The growth rate has been calculated analytically as well as numerically. The graphical comparison provide us a detailed view of unstable regions. The growth rates demonstrate that the mode becomes more unstable, while increasing the value of frequency ratio $(\omega_{pi}/\Omega_c)^2$.

1 Introduction

The subject of heating effects of magnetized plasmas is a deep-rooted topic, from early 1950s with the start of controlled fusion program. The Bernstein mode can be completely absorbed on the wings of the cyclotron resonance [1], [2]. Ion Bernstein wave i.e., a hot plasma wave, utilizes to carry the radio frequency power to heat the tokamak reactor core. Electron Bernstein wave heating and current driven in spherical tokamaks has been explored because the high density and low magnetic field configuration of these machines make the plasma inaccessible to the Ordinary and Extraordinary modes which are used in standard tokamaks [3].

The problem of perpendicularly propagated electron oscillations with external magnetic field has been discussed by Gross [4] and Sen [5]. Gross alleged to find Landau damping whose wavelength is less than the standard Debye length. Later Bernstein [6] find some errors in Gross's [4] conclusion. He calculated the Bernstein mode with Maxwellian distribution function and observed its stability analysis. That work was also treated with the fully ionized small amplitude oscillations in collisionless plasma with the presence of external magnetic field.

Crawford et al. [7] formulated the dispersion relation of Bernstein mode with delta function i.e., transverse electron velocity distribution. This formulation shows that may be unstable wave lead the growing wave phenomena in finite plasmas due to the interaction with slow wave circuits. Even in an infinite plasma, modes couple with each other, leading to wave growth. Later Crawford [8] has predicted theoretically that cyclotron harmonic waves should propagate in warm plasma confined by a magnetic field, which show cutoff and resonance behavior associated with harmonics of the cyclotron frequency and the upper hybrid resonance frequency.

Ram et al. [9] proved that the Bernstein mode can be excited by mode conversion of either an Extraordinary mode or an Ordinary mode. Ketson et al. [10], used weakly relativistic plasmas for producing dispersion relation for the electrostatic Bernstein mode with full momentum dependence of cyclotron frequency. Later Laing et al. [11] showed that these modes are not completely undamped but have a small negative definite imaginary component closest to the rest cyclotron harmonic.

Cairns et al. [1] explained that the Bernstein wave possess high perpendicular wave numbers which reduce trapping. Efthimion [12] explained that electron Bernstein waves have the potential to heat and drive current for high-β plasmas. Deeba et al. [13] has also calculated electron Bernstein mode with (r,q) distribution function. Ali et al. [14] investigated Bernstein mode in relativistic degenerate plasmas. He discussed the cases in non-relativistic and ultra relativistic regime and proved that Bernstein waves and Upper Hybrid oscillations can be modified by increasing the number density.

Crawford [7] and Leuterer [15] reported first time the presence of electron Bernstein wave in a laboratory plasma in 1965 and 1969 respectively. Such waves have also been observed by spacecraft emitted from the magnetized plasma of Jupiter moon, Io. [16] Mace [17] studied the electron Bernstein wave for isotropic kappa distribution function.

Bernstein waves which are electrostatic in nature observed in the electron cyclotron harmonic frequency range, propagate perpendicular to the ambient magnetic field. These waves have been observed in Li neutral

gas release in the solar wind. Meyer-Vernet et al. [18] discussed that the weakly banded emission from the Jupiter magnetosphere and between consecutive gyroharmonics frequency is quasithermal noise in Bernstein wave. Recent observations have been observed by the Voyager spacecraft of electrostatic waves in Jupiter magnetosphere [19]. The electrostatic electron and ion cyclotron harmonic waves have been observed through Voyager II in magnetosphere of Neptune. Electron Bernstein wave generated by a loss cone distribution is scrambled to Neptune parameters and a comparison of theory with the observed electron flux indicates good agreement [20]. These results were based on Voyager data at the outer planets. Bernhard et al. [21] observed the transmission of a high power electromagnetic waves from the HAARP facility in Alaska.

It was assumed that Maxwellian plasma always supports the Bernstein wave, so that the real frequency can be given by the classical Bernstein wave solutions. But the growth rate can determined by very small number of electrons so many types of perpendicular distribution functions can be used [22]. For f_0 we will use the ring distribution function [23, 24, 27], in weakly collisional plasma the ring distribution may be a source of free energy for instabilities, due to effective temperature anisotropies and streaming [25].

$$f_0 = \frac{1}{2\pi\hat{v}_\perp}\delta(v_\perp - \hat{v}_\perp)\delta(\hat{v}_\parallel - v_\parallel) \tag{1}$$

In literature the distribution function has been used for relativistic calculations of Bernstein wave [22, 23, 24, 26]. But evidence of non relativistic formulation is also available [22, 27]. As the parallel part of distribution function is participating in relativistic version of bernstein mode in cold plasma regime but it has no contribution for non relativistic calculation [22].

The layout of paper is as follows: In section II, we use the kinetic theory to calculate the general dispersion relation for magnetized plasma. We derive the analytical expressions for dielectric constant by using ring distribution functions. A brief summary of results and discussions is given in section III.

2 Mathematical Formulation

We follow the general formalism of kinetic theory to evaluate the instability of Bernstein wave in hot magnetized plasma. For Bernstein wave the relevant component of generalized dielectric tensor is [26, 28, 29, 30, 31]

,

$$\epsilon_{xx} = 1 - \sum_{\alpha} \frac{2\pi}{s} m\omega_{p\alpha}^2 \int_{-\infty}^{\infty} dv_{\parallel} \int_{0}^{\infty} v_{\perp} dv_{\perp} \chi_1 \sum_{n=-\infty}^{\infty} \frac{M_{xx}}{(s + ik_{\parallel}v_{\parallel} + in\omega_{c\alpha})} \tag{2}$$

Where $M_{xx} = \frac{n^2}{z_{\alpha}^2} v_{\perp} \left[J_n(z_{\alpha})\right]^2$, $z_{\alpha} = \frac{k_{\perp} v_{\perp}}{\omega_{c\alpha}}$ and $\chi_1 = \frac{\partial f_0}{\partial v_{\perp}} + \frac{i k_{\parallel}}{s} \left(v_{\parallel} \frac{\partial f_0}{\partial v_{\perp}} - v_{\perp} \frac{\partial f_0}{\partial v_{\parallel}} \right)$, s=-$i\omega$

Since we are dealing with perpendicular propagation so $k_{\parallel} = 0$ so $\chi_1 = \frac{\partial f_0}{\partial v_{\perp}}$. Where $\omega_{p\alpha}$ and $\omega_{c\alpha}$ are plasma and gyro frequencies respectively and α shows the species i.e., electron and ion as well.

By simplifying we get

$$1 + \sum_{\alpha} \frac{4\pi\omega_{p\alpha}^2 m^2}{k_{\perp}^2} \sum_{n=1}^{\infty} \frac{n^2\omega_{c\alpha}^2}{(\omega^2 - n^2\omega_{c\alpha}^2)} \int_{-\infty}^{\infty} dv_{\parallel} \int_{0}^{\infty} dv_{\perp} J_n^2(z_{\alpha}) \frac{\partial f_0}{\partial v_{\perp}} = 0 \tag{3}$$

Where f_0 is distribution function and in this case the ring distribution function has been used

$$f_0 = \frac{1}{2\pi\hat{v}_{\perp}} \delta(v_{\perp} - \hat{v}_{\perp}) \delta(\hat{v}_{\parallel} - v_{\parallel})$$

As the parallel streaming has no effect on nonrelativistic ion Bernstein mode so we obtain the dispersion relation for Bernstein wave after performing simple integrations, as the

$$1 - \sum_{\alpha} \frac{\omega_{p\alpha}^2}{\omega^2} \sum_{n=1}^{\infty} \frac{2n^2 J_n(\hat{z}_{\alpha}) J_n'(\hat{z}_{\alpha})}{\hat{z}_{\alpha}} \left[\frac{2\omega^2}{(\omega^2 - n^2\omega_{c\alpha}^2)} \right] = 0 \tag{4}$$

At lower frequency range, the harmonics of the ion cyclotron frequency, with similar properties exhibits as that of electron Bernstein wave. The ion contribution in dispersion relation can be neglected at high frequency range, but the electron contribution persist even at low frequencies. So there is not a complete symmetry between the two types of Bernstein waves [30]. Opening the sum over species $\sum_{\alpha}$ for electrons and ions:

$$\begin{aligned} 1 = & \frac{\omega_{pe}^2}{\omega^2} \sum_{n\,=\,1}^{\infty} \frac{2n^2 J_n\left(\hat{z}_e\right) J_n'\left(\hat{z}_e\right)}{\hat{z}_e} \left(\frac{2\omega^2}{\omega^2 - n^2\omega_c^2} \right) \\ & + \frac{\omega_{pi}^2}{\omega^2} \sum_{n\,=\,1}^{\infty} \frac{2n^2 J_n\left(\hat{z}_i\right) J_n'\left(\hat{z}_i\right)}{\hat{z}_i} \left(\frac{2\omega^2}{\omega^2 - n^2\Omega_c^2} \right) \end{aligned} \tag{5}$$

Where ω_c represents the electron gyro frequency and Ω_c is ion gyro frequency, ω_{pe}^2 and ω_{pi}^2 are plasma frequencies for electrons and ions respectively. The value of $J_n'(\hat{z}_{i,e})$ as $\hat{z}_{i,e} \to 0$ is given as $J_n'(\hat{z}_{i,e}) = \frac{n}{\hat{z}_{i,e}} J_n(\hat{z}_{i,e})$, for electrons $\hat{z}_e = \frac{k_\perp \hat{v}_\perp}{\omega_c}$ and for ions $\hat{z}_i = \frac{k_\perp \hat{v}_\perp}{\Omega_c}$, By applying the small $\hat{z}$ argument expansion as $\hat{z} \to 0$, and according to Chen [30] we consider only n = 1 term

$$1 = \frac{\omega_{pe}^2}{\omega^2 - \omega_c^2} + \frac{\omega_{pi}^2}{\omega^2} \sum_{n\,=\,1}^{\infty} \frac{2n^2 J_n(\hat{z}_i) J_n'(\hat{z}_i)}{\hat{z}_i} \left(\frac{2\omega^2}{\omega^2 - n^2\Omega_c^2} \right) \tag{6}$$

By applying these approximation, first part of eqn. 6 , reduces to upper hybrid mode as explained by Bashir et al. [22]. By following Chen [30] separate out the n = 1 term for Ion Bernstein mode, we obtain

$$1 = \frac{\omega_{pe}^2}{\omega^2 - \omega_c^2} + \frac{\omega_{pi}^2}{\omega^2 - \Omega_c^2} + \frac{\omega_{pi}^2}{\omega^2} \sum_{n\,=\,2}^{\infty} \frac{2n^2 J_n(\hat{z}_i) J_n'(\hat{z}_i)}{\hat{z}_i} \left(\frac{2\omega^2}{\omega^2 - n^2\Omega_c^2} \right) \tag{7}$$

This result is in good agreement with Maxwellian results of Chen [30].

.

3 Results and discussion

By numerically solving eqn. 7, we can separate the real and imaginary parts of the wave as $\omega = \omega_r + i\omega_i$. The imaginary part plays a significant role in estimating the threshold value and determining the purely growing mode i.e:, $\omega_r = 0$ [32, 33, 34].

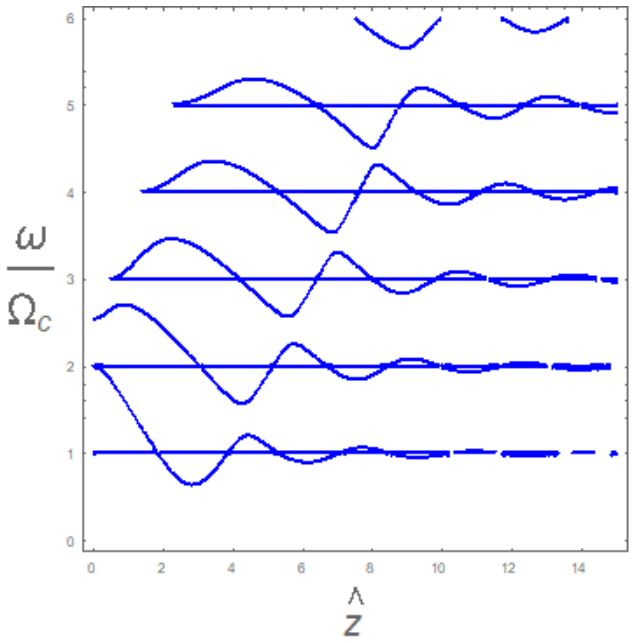

Fig. 1: The relation of ω_r/Ω_c and $\hat{z}$ for $\omega_{p_i}^2/\Omega_c^2 = 11.0$.Where $\hat{z}$=$k_\perp \hat{v}_\perp/\Omega_c$,is function of wavelength and magnetic field.

The fig.1 shows the stability of the ion Bernstein mode for ω_r/Ω_c vs $\hat{z}_i = k_\perp \hat{v}_\perp/\Omega_c$,showing that at ω_{pi}^2/Ω_c^2=11.0 the wave is stable but fig. 2 shows that the variation of frequency range in real part of wave, which create intersection of branches. The first intersection point can easily be observed at $\omega_{p_i}^2/\Omega_c^2$=11.5, this is the threshold value for instability of the ion Bernstein wave. During overlapping of wave branches in real frequency, the wave becomes unstable and gaps are generated between the harmonics which was discussed by Bashir et al.[22]. According to Bashir et al [22] and Crawford [35], the threshold point for electron Bernstein wave is $\omega_{p_e}^2/\omega_c^2$ =6.63 while for ion Bernstein wave the threshold value is $\omega_{p_i}^2/\Omega_c^2 = 11.5$ where $\omega_{p_i}^2/\Omega_c^2$and $\omega_{p_e}^2/\omega_c^2$ are plasma to gyro frequencies ratio. The comparison of electron Bernstein mode with the ion Bernstein mode yields that ion try to shift threshold values at weak magnetic field.

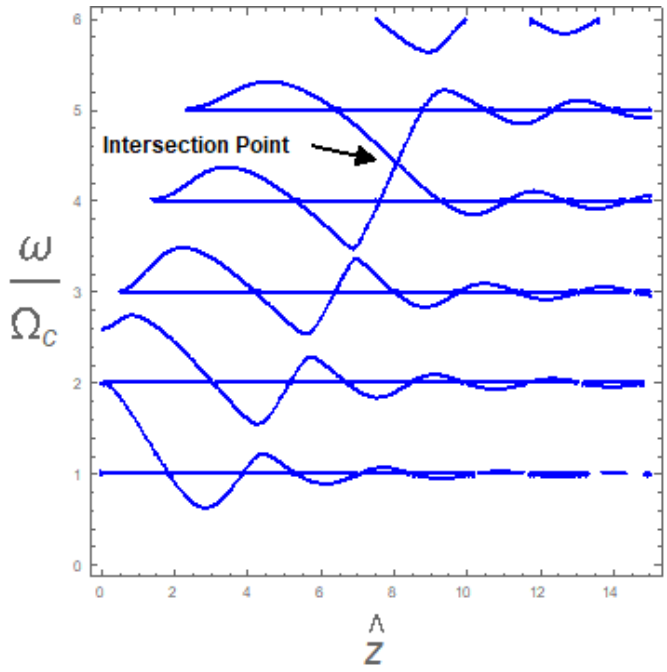

Fig. 2: The relation of ω_r/Ω_c and $\hat{z}$ for $\omega_{p_i}^2/\Omega_c^2 = 11.5$.The harmonics start overlap where $\hat{z}$=$k_\perp \hat{v}_\perp/\Omega_c$

At $\omega_{pi}^2/\Omega_c^2 = 12$, the wave is unstable and gaps generated between the harmonics become more prominent as we can observe in fig. 3. Now for revealing the fact of gaps between harmonics by plotting complex part of frequency as we have already considered $\omega = \omega_r + i\omega_i$, it tells about the imaginary part ω_i of wave which is disappeared on real frequency scale. The study of this complex part of frequency gives an important result that the wave is growing in these specific regions. It means that the instability like electron bernstein mode, the ion Bernstein mode is also unstable for the ω_{pi}>Ω_c however the numerical threshold value is greater than electron Bernstein wave. In the figures that follow, the solid lines show the real part and the dashed lines represent the imaginary part of the wave frequency ω.

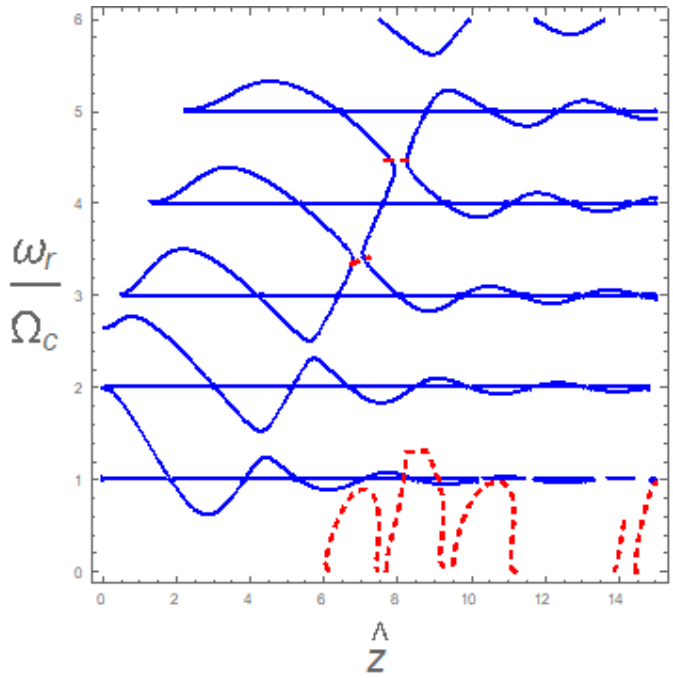

Fig.3 : The relation of ω_r/Ω_c and $\hat{z}$ for $\omega_{p_i}^2/\Omega_c^2 = 12.0$.In fig. the dotted red lines within the harmonics show the unstable regions.

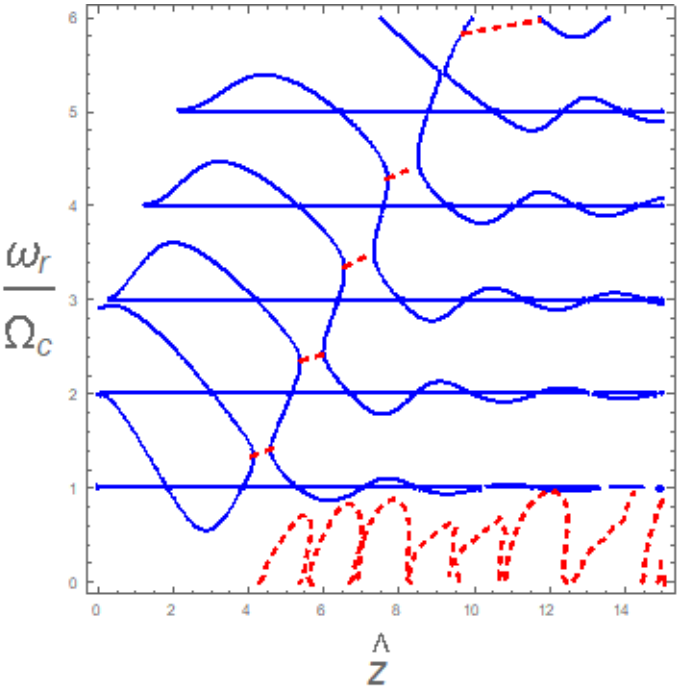

Fig.4: The relation of ω_r/Ω_c and $\hat{z}$ for $\omega_{p_i}^2/\Omega_c^2 = 15.0$.In fig. the dotted red lines within the harmonics show the unstable regions.

The results obtained on increasing the value of ratio ω_{pi}^2/Ω_c^2 from 12 to 15 are displayed in fig.4. These results can be directly compared with Bashir et al.[22] and Crawford [32]. The comparison reveals that the real frequency structure is similar, unstable regions can be observed between the harmonics. The appearance of this inter branches instability becomes more frequent as we increase the value of ω_{pi}^2/Ω_c^2. Fig. 5 shows a group of inter branches instability. There are unstable regions between the harmonics for shorter wavelength area. One of them is a nonresonating or purely growing mode for which $\omega_r = 0$ [32, 33, 34]. This mode occurs due to augmentation of amplitude but not with overlapping. In fig. 5, it has been noticed that unstable regions are less growing and purely growing mode has small domain. Fig. 5 and 6 show harmonics for $\omega_{pi}^2/\Omega_c^2 = 50$ and $\omega_{pi}^2/\Omega_c^2 = 60$ respectively. With higher values of ω_{pi}^2/Ω_c^2, the domain of purely growing mode is also increasing. One can also observe that the instabilities are effected by value of magnetic field. With decreasing the value of magnetic field, anisotropy increases, which agrees with high frequency Bernstein mode instability case [22].

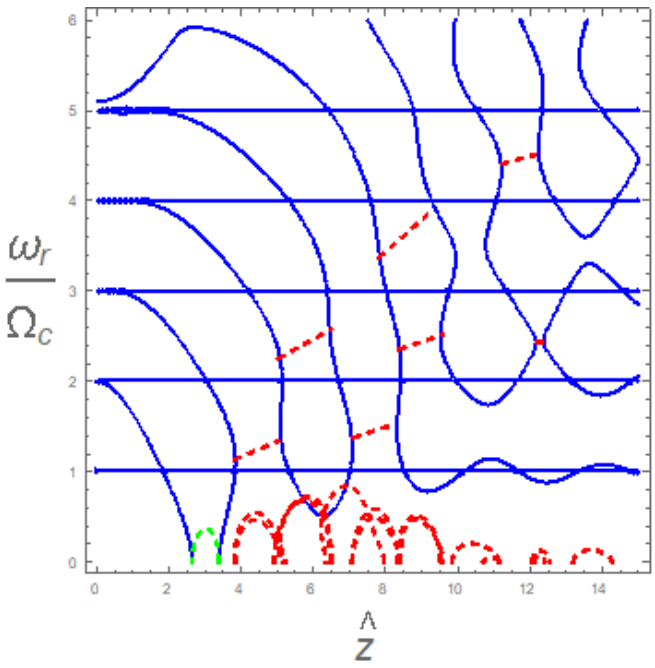

Fig. 5: The relation of ω_r/Ω_c and $\hat{z}$ for $\omega_{p_i}^2/\Omega_c^2 = 50$. The red dotted lines within the harmonics show the unstable regions and their respective imaginary part is in red color. The green color shows the purely growing part where $\omega_r = 0$.

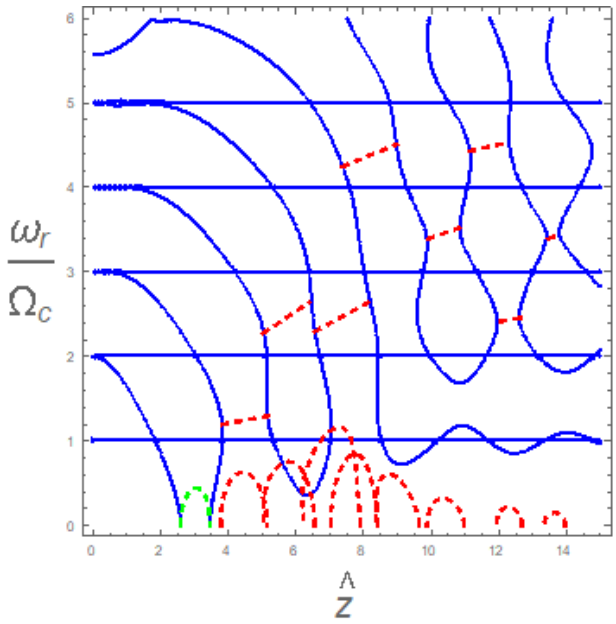

Fig. 6: The relation of ω_r/Ω_c and $\hat{z}$ for $\omega_{p_i}^2/\Omega_c^2 = 60$. The trend is same as in fig. 5, the purely growing mode where $\omega_r = 0$ is in green color.

Above discussion draws a complete picture of instabilities at different values of argument. On comparison with the electron Bernstein wave, the ion Bernstein wave has high threshold value with low frequency. A direct correlation between value of ω_{pi}^2/Ω_c^2 and overlapping of wave branches shows that the instability grows with the decreasing value of magnetic field and the wave becomes unstable for high density. The distribution function provides free energy which is cause of wave instability. Nsengiyumva et al. [25] discussed the ion Bernstein mode with kappa distribution function and according to [25], the unstable regions shifted to higher wavenumber or lower wavelength by decreasing kappa (κ_i), this is in good agreement with the results of ring velocity distribution function. This comparison shows that the ring velocity distribution reveals the instability of Bernstein mode earlier than kappa distribution function. Bernstein mode is current driven mode and produces heating effect [36, 37, 38]. In pulsars, electrostatic waves are observed and there are number of trapped modes present in pulsars. This discussion will be useful in any future treatment of radiation data from pulsars.

References

[1] Cairns R. A. 2003 Spherical Tokamak Workshop 2003 Bernstein Mode Heating and Current Drive

[2] Ram A. K. 2003 30th EPS Conference on Controlled Fusion and Plasma Phys., St. Petersburg , ECA **27** A, P-3. 204
[3] McGregor D. E., Cairns R. A, Lashmore-Davies C. N., O'Brien M. 2004 31st EPS Conference on Plasma Phys. London, 28 June - 2 July 2004 ECA, **28** G, P-1.108
[4] Gross E. P. 1951 Phys. Rev. **82**, 232
[5] Sen H. K. 1952 Phys. Rev. **88**, 816
[6] Bernstein I. B. 1958 Phys. Rev. **1,** 09
[7] Crawford F. W., Tataronis J. A. 1965 J. App. Phys, **36 ,** 2930
[8] Harker K. J., Crawford F. W. 1968 J. Appl. Phys. **39**, 5959
[9] Ram A. K., Bers A., Lashmore-Davies C. N. 2002 Phys. Plasmas, **9,** 409
[10] Ketson D. A., Laing E. W., Diver D. A. 2003 Phys. Rev. E 6**7**, 036403
[11] Laing E. W., Diver D. A. 2005 Phys. Rev. E **72**, 036409
[12] Efthimion P. C., Hosea J. C., Kaita R., Majeski R., Taylore G. 1999 Rev. Sci. Instrum. **70**, 1018
[13] Deeba F., Murtaza G. 2010 Phys. Plasmas **17**, 102114
[14] Ali M., Hussain A., Murtaza G. 2011 Phys. Plasmas **18**, 092104
[15] Leuterer F. 1969 Phys. Plasma **11**, 615
[16] Moncuquet M., Meyer-Vernet N., Hoang S. 1997 J. Geophys. Res. **102**, 03313
[17] Mace R. L. 2003 Phys. Plasmas **10**, 2181
[18] Meyer-Vernet N., Hoang S., Moncuquet M. 1993 J. Geophys. Res. **98**,21163
[19] Barbosa D. D., Kruth W. S. 1980 J. Geophys. Res. **85**, 08981
[20] Barbosa D. D., W. S. Kruth, Gurnett D. A. 1993 J. Geophys. Res. **98,** 19465-19469
[21] Bernhard P. A., Selcher C. A., Kowtha S. 2011 J. Geophys. Res. Lett. **38**, 19107
[22] Bashir M. F., Noreen N., Murtaza G., Yoon P. H. 2014 Phys. Plasma and Cont. Fusion, **56,** 055009
[23] Wu C. S., Krauss-Varban D. Huo T. S. 1988 J. GeoPhys. Res. **93**, 11527
[24] Gary S. P., Madland C. D. 1988 J. GeoPhys. Res. **93**, 235
[25] Nsengiyumva F., Mace R. L., Hellberg M. A. 2013 Phys. Plasmas, **20,** 102107
[26] Montgomery D.C., Tidman D.A. 1964 *Plasma Kinetic Theory*, McGraw-Hill Press, New York, USA
[27] Vandas M., Hellinger P. 2015 Phys.Plasmas, **22**, 062107
[28] Fredricks R. W. 1971 J. Geophys. Res. **76**, 5344
[29] Yoon P. H., Davidson R. C. 1987 Phy. Rev. A Gen Phys., **35**, 2619

[30] Chen F. F. 1984 *Introduction to plasma physics and controlled fusion,* Plenum publishing Corporation 233 spring street, New York, USA
[31] Krall N. A., Trivelpiece A. W. 1973 *Principles of Plasma Physics*, McGraw-Hill Book Company, New York, USA
[32] Lazar M., Poedts S., Shlickeiser R., Ibscher D. 2013 arXiv:1307.0768v1 [astro-ph.SR]
[33] Davidson R. C., Wu C. S., 1970 Phys. Fluids, **13**, 1407
[34] Hadi F., Yoon P. H., Qamar A., 2015 Phys. Plasmas, **22**, 022112
[35] Crawford F. W. 1965 Radio Sci. J. Res. (NBS/USNC-URSI), **69D**, 789
[36] Laqua H. P., Andruczyk D., Maresen S., Otte M., Podoba Y. Y., Preinhealter J., Urban J. 2007
[37] Kuwahata A., Igami H., Kawamori E., Kogi Y., Inomoto M., Ono Y. 2014 Phys. Plasmas, **21**, 102116
[38] Ram A. K., Bers A. 2002 Phys. Plasmas, **09**, 409